Non-Steady-State Diffusion in a Multilayered Tissue Initiated by Manipulation of Chemical Activity at the Boundaries

Irving Fatt,* Claude J. Giasson,#§ and Thomas D. Mueller
*School of Optometry, University of California, Berkeley, California 94720-2020 USA; #Ecole d'Optométrie, Université de Montréal, Montréal, Québec, Canada; and §Research Unit in Ophthalmology, Hôpital Maisonneuve-Rosemont, Montréal, Québec, Canada

ABSTRACT Diffusion of ionic and nonionic species in multilayered tissues plays an important role in the metabolic processes that take place in these tissues. To create a mathematical model of these diffusion processes, we have chosen as an example hydrogen-bicarbonate ion pair diffusion within the mammalian cornea. This choice was based on the availability of experimental data on this system. The diffusion coefficient of the hydrogen-bicarbonate ion pair in corneal stroma and epithelium is calculated from the observed change in pH in the stroma when conditions at the corneal anterior epithelial surface are changed while the posterior surface is continually bathed with a Ringer's solution in equilibrium with a CO_2-gas air mixture. Matching experimental results to a mathematical model of the cornea as a two-layer diffusion system yields, at 37°C, a diffusion coefficient of the hydrogen-bicarbonate ion pair of 2.5×10^{-6} cm^2/s in the stroma and 0.4×10^{-6} cm^2/s in the epithelium. Application of the Nernst-Einstein equation to these data gives the following diffusion coefficients in the two layers: 1) stroma, $D(H^+) = 11.8 \times 10^{-6}$ cm^2/s; $D(HCO_3^-) = 1.5 \times 10^{-6}$ cm^2/s; and 2) epithelium, $D(H^+) = 1.9 \times 10^{-6}$ cm^2/s; $D(HCO_3^-) = 0.22 \times 10^{-6}$ cm^2/s.

INTRODUCTION

Animal tissues are almost always multilayered. Arteries and veins have an outer coat that surrounds a muscular coat. Within the muscular coat is an elastic white fibrous tissue that is lined with endothelial cells. The alimentary canal is essentially a tube whose walls are fashioned from four layers of tissue: a mucous lining, a submucous coat of connective tissue, a muscular coat, and a fibrous coat. The details of these layers vary from the mouth to the end of the intestinal tract, but the layered structure remains constant.

The tissues noted above offer resistance to the diffusion of ionic and nonionic species that must move into and out of the whole organism so it can remain viable. Diffusional resistance depends on the species that is diffusing and on the nature of the tissue layer in which the diffusion is taking place. In a multilayered tissue, the diffusional resistance for a given diffusing species will usually be different in the individual layers.

The diffusional transport rate of a species may be independent of time, or if conditions within the system change with time, the transport rate can become time dependent. Information concerning the metabolic mechanism operating within a tissue can often be obtained by a detailed examination of diffusion rates within the individual layers of a multilayered tissue. In this paper we demonstrate how time-dependent diffusion data can be combined with a computer-generated model of diffusion in a multilayered system to arrive at diffusion coefficients in the individual layers.

We have chosen to base our mathematical model of non-steady-state diffusion on the layered cornea of the mammalian eye. This tissue can be treated as having one-dimensional diffusion, because its area is large compared to its thickness. Its main individual layers, well characterized by previous histological studies, are as follows: epithelial cells on the anterior surface, a tough fibrous stroma that gives shape to the cornea, and a posterior layer of nonvascular endothelial cells.

The diffusing species chosen is the hydrogen ion-bicarbonate ion pair. This diffusing species was chosen because Giasson (Giasson, 1994; Giasson et al., 1995) and coworkers have presented extensive data on time-dependent pH changes in the cornea that are created when acidity at the anterior or posterior surface is changed. These pH changes can be interpreted in terms of the diffusion coefficient of the hydrogen-bicarbonate ion pair, and the individual diffusion coefficients of hydrogen ion and bicarbonate ion in both the stroma and epithelium.

METHODS

Experimental

Giasson (Giasson, 1994; Giasson et al., 1995) has collected data on corneal pH that can be mathematically analyzed to yield an estimate of the diffusion coefficient of the H^+-HCO_3^- ion pair in the excised rabbit corneal stroma and epithelium. The pH-sensitive dye 2′,7′-bis(2-carboxyethyl)-5-(and -6) carboxyfluorescein (BCECF-AM) was loaded into rabbit endothelial cells while the excised cornea was held in a perfusion cell described previously (Klyce et al., 1973; Giasson, 1994).

Two separate experimental conditions were used in these experiments. Under both conditions, fluorescence from the endothelial layer was continually monitored to yield a record of decrease in pH after a change in condition at the anterior surface. In the first case, the posterior surface of

Received for publication 27 February 1996 and in final form 25 September 1997.

Address reprint requests to Dr. Claude J. Giasson, Ecole d'Optométrie, Université de Montréal, CP 6128, Succursale Centre-Ville, Montréal, Québec H3C 3J7, Canada. Tel.: 514-343-5946; Fax: 514-343-2382; E-mail: giassonc@ere.umontreal.ca.

0006-3495/98/01/475/12 $2.00

a rabbit cornea was continually perfused at 37°C with a HCO_3^--rich Ringer's solution (Table 1) equilibrated with a 5% carbon dioxide/95% air gas mixture. The anterior surface of the cornea was in contact with air. After pH was noted to be independent of time in the endothelial cell layer, the anterior surface of the cornea was covered at time 0 by a tight-fitting, gas-impermeable polymethylmethacrylate (PMMA) contact lens (central thickness 0.17 mm). In the experimental arrangement there is, until time 0, a steady-state diffusion of CO_2 from the posterior to the anterior surface. At times later than 0, the CO_2 cannot escape at the anterior surface, so the CO_2 partial pressure increases within the tissue until it is uniform from the anterior to the posterior surface and becomes equal to the partial pressure of CO_2 present at the posterior surface. The small amount of CO_2 produced by the stromal and epithelial cell can be ignored (Fatt and Weissman, 1992).

In the second set of experiments, the epithelium and endothelium, respectively, were perfused with HCO_3^--free and HCO_3^--rich buffer solutions (Table 1). At time 0, the epithelial perfusate was switched from the air-equilibrated HCO_3-free solution to a 5% CO_2-HCO_3^- solution, causing the pH observed in the endothelial cell layer to drop by ~0.17 pH units as the tissue was acidified by the 5% CO_2-HCO_3^- Ringer's solution applied at the epithelial surface.

The fluorophotometer has been described previously (Bonanno and Machen, 1989; Bonanno and Giasson, 1992). The pH measuring system of the fluorometer is based on the observed relationship between pH and the ratio of fluorescence at two wavelengths. The illumination is provided by a xenon arc lamp of the epifluorescence attachment mounted on a Nikon Diaphot inverted microscope. The dye was excited by light passing through 440-nm and 490-nm interference filters of 20 nm and 10 nm half-bandwidth. The filters, mounted on a polarized filter shuttle, were placed alternately in the light path once every second to give 1 ratio/s. The light was focused on endothelial cells by a long-working-distance (10.5 mm), 10× objective (NA 0.25; Nikon). The light emitted from the fluorescent dye in the endothelium was passed through a barrier filter (520–560 nm) and then directed to a photomultiplier tube, the digital output of which was stored in a PC computer.

Fig. 1 shows a record of the pH output signal from these two sets of experiments after smoothing by a computer program. Fig. 2 shows the same data as in Fig. 1, but converted to hydrogen ion chemical activity through the defining equation for pH, namely,

$$\mathrm{pH} = -\log a(\mathrm{H}^+) \tag{1}$$

MATHEMATICAL STATEMENT OF THE PROBLEM

The mathematical analysis of the diffusion problem under study here assumes simple Fickian diffusion in a one-dimensional body. There are assumed to be no sources or sinks for hydrogen or bicarbonate ion, other than the very rapid decomposition of carbonic acid introduced into the tissue as dissolved carbon dioxide gas. Reaction of hydrogen or bicarbonate ion with the corneal tissue is limited to the case of instantaneous reversible reaction.

TABLE 1 Composition of the Ringer's solution (mM)

	HCO_3^-	HCO_3^--free
Na^+	143.5	143.5
K^+	4	4
Mg^{2+}	0.6	0.6
Ca^{2+}	1.4	1.4
$NMDG^+$	0	0
Cl^-	118.2	118.2
HPO_4^{2-}	1	1
HEPES	10	10
MES	0	0
$Gluconate^-$	1.4	29.9
HCO_3^-	28.5	0
Glucose	5	5
pH	7.5	7.5
CO_2	5%	0%

NMDG, *N*-Methyl-D-glucamine; MES, 2-(*N*-morpholino)ethanesulfonic acid.

A discussion of multiion diffusion that includes the diffusion coefficients of the various ions and reactions among them in dilute solutions has been given by Newman (1991). An exact mathematical analysis as given by Newman is not possible for the cornea, because the physical properties of the cornea needed to make the complete analysis are not available. Instead of seeking an exact and complete solution of the problem of diffusion in the cornea, we shall use a mathematical model that allows the observed data to be fitted by only two parameters, namely, the diffusion coefficient of the H^+-HCO_3^- ion pair in the stroma and epithelium. From these two parameters, we shall proceed, by means of the Nernst-Einstein equation (Newman, 1991), to calculate the diffusion coefficients of the individual ions. We chose in this paper not to include any active processes, because they are not encompassed in the purely diffusional model we develop. We chose instead to rely on the concept of Occam's Razor—we will introduce the minimum number of parameters necessary to fit the observations to the model.

The problem of a diffusing species becomes complex when the dissolved species is a salt that ionizes into independently mobile ions. Newman points out that the condition for electroneutrality within the solution requires that positive and negative ions move together in a concentration gradient, so diffusion of an ion pair can be treated as the diffusion of the un-ionized salt (Newman, 1991). He also points out that treating the diffusion problem as that of a single un-ionized dissolved substance eliminates the need for knowledge of the chemical activity coefficients of the individual ions and therefore leads to an unambiguous and easily defined diffusion coefficient. This diffusion coefficient is not that of either the cation or anion, but is, instead, an average coefficient weighted by the charge on each ion. As will be shown later, we have used some reasonable assumptions to calculate the individual ion diffusion coefficients from the observed ion pair diffusion coefficient by means of the Nernst-Einstein relationship.

In the diffusion studies presented here, the concentrations and chemical activities of H^+ and HCO_3^- are known only for regions outside the cornea, because the partition coefficients for the ions in corneal tissues are not known. However, at the outer boundaries, where the perfusing fluid is in contact with the cornea, there is the thermodynamic requirement that the chemical activity be the same in the perfusing fluid and in the tissue immediately adjacent to the boundary. There is also the thermodynamic requirement that the chemical activity at all times must be the same on the stroma-epithelium interface if these tissues are treated as homogeneous bodies, thereby ignoring their cellular structure.

The mathematical model proposed here treats the cornea as composed of two homogeneous, cell-free layers: the

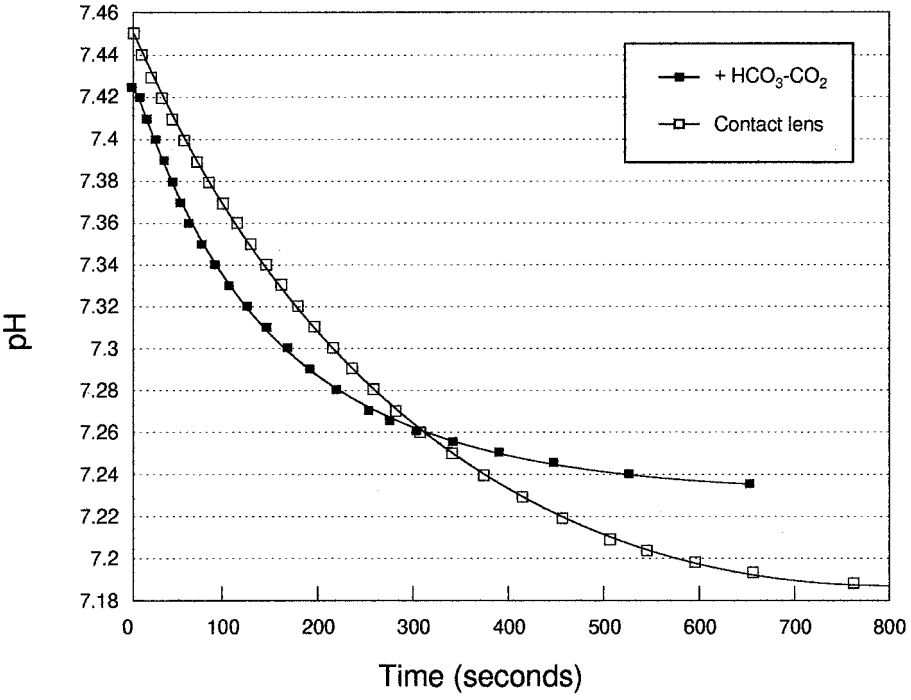

FIGURE 1 pH output signal of the corneal endothelium after smoothing by a computer program. At time 0, a contact lens was inserted (□), or the Ringer's solution superfusing the epithelium was switched from a HCO_3^--free to a 5% CO_2-HCO_3^- Ringer's (■).

stroma and epithelium. The endothelium, 5–10 μm thick, where the change in pH is monitored, is treated as a layer with the same properties as the stroma. Because the endothelium is so thin, the separate contribution of this layer to diffusion dynamics is believed to be minimal. As will be shown presently, even the much thicker epithelium has only a relatively small effect on diffusion dynamics under certain boundary conditions. Furthermore, calculations that lead to a match of the model to the observed pH versus time data show that the experimental results are not sensitive to the location of the pH monitoring dyed layer, as long as that layer is within a region 10–20 μm from the posterior surface. The model therefore uses the assumption that the experimentally observed, time-dependent pH is due entirely to diffusion dynamics in the stroma and epithelium.

During the period of equilibration, before the experiment is begun, the endothelial surface is at an HCO_3^- chemical activity established by a 5% CO_2/95% air Ringer's solution.

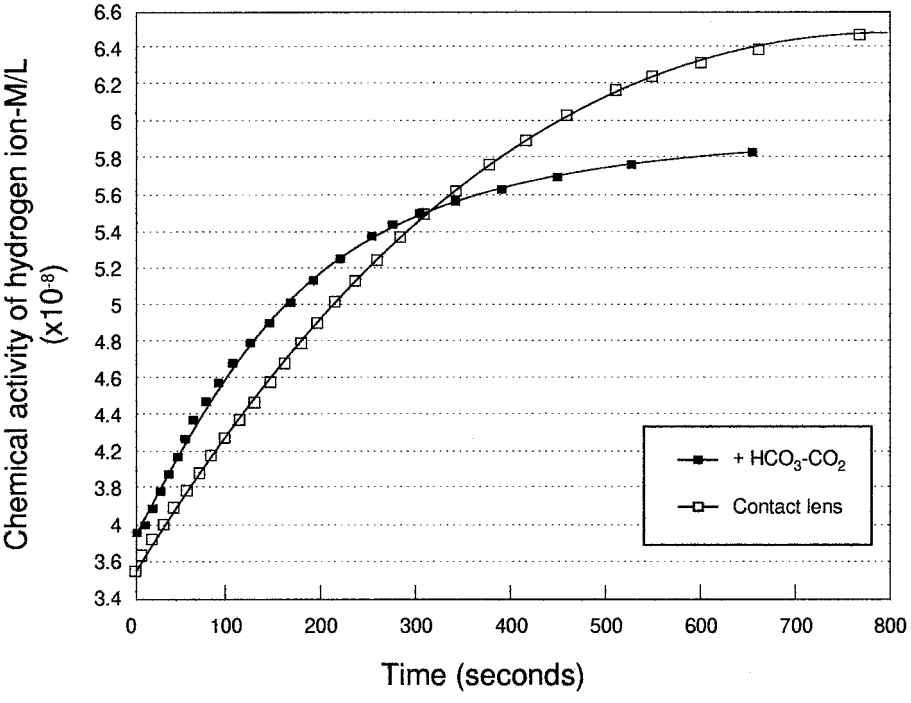

FIGURE 2 Data of Fig. 1 converted to hydrogen ion chemical activity. Symbols are as in Fig. 1.

During this period the anterior surface (epithelium) is in equilibrium with air in which the CO_2 chemical activity is close to zero. We assume that there is a linear gradient in HCO_3^- chemical activity in the stroma and epithelium from a high value at the posterior surface to a lower value at the anterior surface. The fluorescence is observed at a point that is some small distance from the posterior boundary. It must be borne in mind that the changes in fluorescence observed during the experiment must mean that the dye-loaded cells are at a finite distance from the mathematically established posterior boundary at $X = 0$. If the dye-loaded cells were exactly at $X = 0$, then no change in fluorescence would be observed, because the surface at $X = 0$ is flooded continuously with the 5% CO_2/95% air Ringer's solution, in which the H^+ and HCO_3^- chemical activities remain constant with time. We will show later that the mathematical model does not require that we know exactly where the fluorescent probe is located, as long as the probe is within 80 μm of $X = 0$.

For both sets of experiments, the initial (time 0) steady-state profile of the chemical activity of the H^+-HCO_3^- ion pair in the cornea is as shown in Fig. 3. For times greater than zero in the first set of experiments, the anterior surface of the cornea is covered by a tight-fitting PMMA contact lens. Under this condition, there can be no diffusion of any of the diffusing species across the surface at $X = L$. This condition can be written as

$$\left(\frac{da}{d\chi}\right)_{\chi=L} = 0 \qquad (2)$$

The change in chemical activity of the H^+-HCO_3^- ion pair, as calculated from the model, is shown in Fig. 4. The change in H^+-HCO_3^- chemical activity that is observed as a change in pH is the result of release of hydrogen ion from the reaction of dissolved carbon dioxide and water, according to the reaction

$$CO_2 + H_2O = H_2CO_3 = HCO_3^- + H^+$$

HCO_3^- does not decompose to CO_3^{2-} and another H^+ under physiological conditions (Davenport, 1958). The reaction of carbon dioxide and water to form carbonic acid and the reverse reaction are rapid because they are catalyzed by the carbonic anhydrase catalyst, assumed to be uniformly present in the cornea, although in reality carbonic anhydrase is concentrated in epithelial and endothelial cells and in the stroma (Wistrand et al., 1986; Conroy et al., 1992). In the time frame of the experiment, the carbon dioxide-water reaction is expected to be always at equilibrium. The mathematical model makes the assumption that at every point in the cornea, there is local equilibrium between hydrogen ion and bicarbonate ion (Davenport, 1958). Therefore a time-dependent measurement of hydrogen ion activity (pH) will yield the time-dependent changes in H^+-HCO_3^- ion pair chemical activity. H^+-HCO_3^- ion pair chemical activity is established at the posterior surface by a Ringer's solution that is in equilibrium with 5% carbon dioxide gas/95% air. This solution will have 96% of the carbon dioxide in the form of bicarbonate ion, with the remainder as dissolved carbon dioxide gas (Davenport, 1958).

When there is diffusion of a single dissolved species in one dimension across a homogeneous layer, the mathematical treatment that gives concentration as a function of time and position is usually not very complicated. The problem is especially simple if, as an initial condition, we know the concentration of the diffusing species at some point.

In our study of ionic diffusion (hydrogen and bicarbonate ions) in the cornea, we do not have a homogeneous layer that would allow concentration to be used in place of chemical activity. The experimental arrangement allows us to know the concentration of ions and dissolved carbon dioxide in the perfusing solution but not in the corneal tissue. By assuming instantaneous chemical equilibrium across the various boundaries in our system, we know from thermodynamic considerations that chemical activity must be equal across every boundary for all species. In the initial condition of both sets of experiments performed in this study, the posterior surface of the excised cornea was perfused with Ringer's solution equilibrated with a gas of 5% carbon dioxide/95% air (v/v). The anterior surface was open to moist air or perfused with a Ringer's solution equilibrated with air.

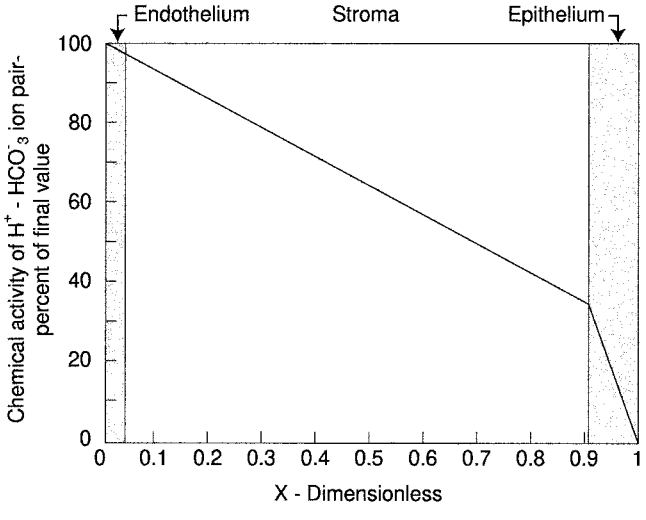

FIGURE 3 Steady-state profile of CO_2 chemical activity in the cornea before a change in boundary condition is imposed at the anterior surface.

MATHEMATICAL MODEL

Diffusion of the solute, the H^+-HCO_3^- ion pair, can be described by a simplified form of the more general set of equations if we assume that there is no reaction of diffusing material with the substrate through which it diffuses. This assumption can be examined later in terms of its effect on the calculated diffusion coefficient. A further assumption is that the diffusing species is neither generated nor consumed

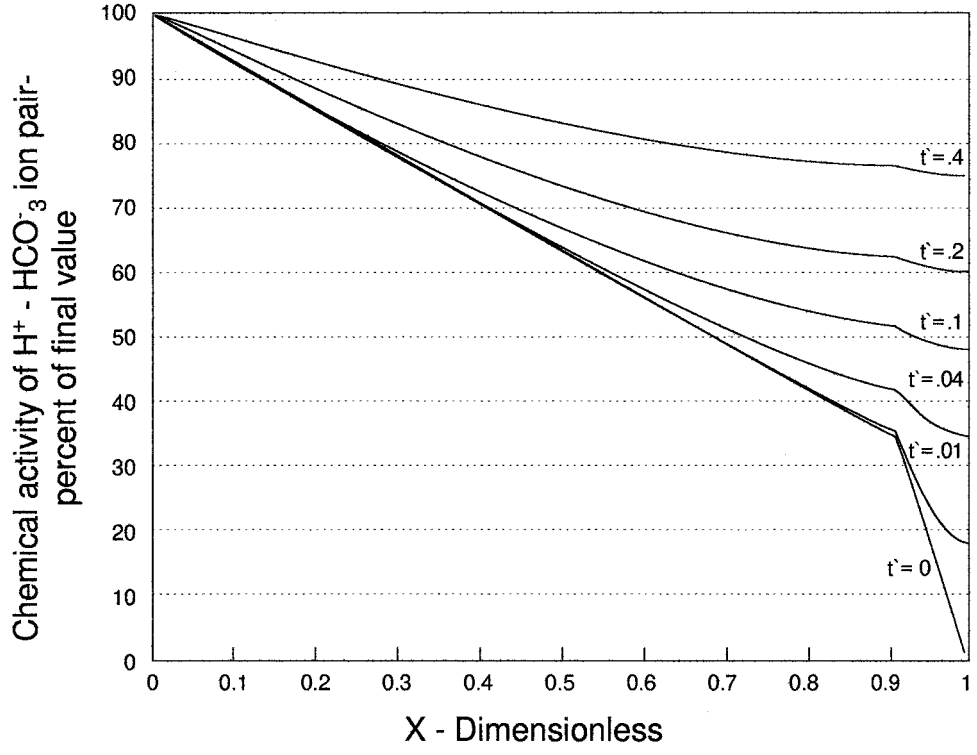

FIGURE 4 Computer-calculated profile of the H^+-HCO_3^- ion pair chemical activity as a function of time in the stroma, from $x = 0$ to $x = 0.9$, and epithelium ($x = 0.9$ to $x = 1.0$). The parameter on the curves is t', taken to be equal to Dt/L^2. Before $t = 0$, there was steady-state diffusion of H^+ and HCO_3^- from the posterior to the anterior surface. For times greater than $t = 0$, the anterior surface is closed with an impermeable contact lens.

by the solvent or solid substrate. With these assumptions we can write a simple form of Fick's law for non-steady-state diffusion in each of the two layers, stroma and epithelium, of the model cornea. For the two layers these equations are

$$\left(\frac{\partial a}{\partial t}\right)_s = D_s\left(\frac{\partial^2 a}{\partial \chi^2}\right) \tag{3}$$

$$\left(\frac{\partial a}{\partial t}\right)_e = D_e\left(\frac{\partial^2 a}{\partial \chi^2}\right) \tag{4}$$

where a is chemical activity, t is time, x is distance, and D is a diffusion coefficient that is the Nernst-Einstein combination of the hydrogen and bicarbonate ion diffusion coefficients for a solution of the ions held within a nonreactive porous matrix. Subscripts s and e refer to stroma and epithelium, respectively. Equations 3 and 4 are written for only one dimension because of the assumption of a cornea that is very thin relative to its lateral dimension.

Equations 3 and 4 can, in theory, be integrated if one initial condition in time and two boundary conditions in the spatial coordinate X are specified for each equation.

For time 0, the initial condition, we take the condition at $x = 0$ as the bicarbonate ion chemical activity in the solution bathing the posterior surface of the cornea. At $x = L$, the anterior surface of the cornea, the bicarbonate ion chemical activity is at some lower value, because in the experimental arrangement the anterior surface is in contact with air or with a solution equilibrated with air. In both cases, the carbon dioxide content is very low. At $x = h$, the interface between stroma and epithelium, the initial bicarbonate ion chemical activity is given by the steady-state form of Fick's diffusion law. In the stroma and epithelium, the steady-state distributions at time 0 are

$$a_s(\chi) = a_0 - D_s\left(\frac{da}{d\chi}\right)_s \tag{5}$$

$$a_e(\chi) = a_h - D_e\left(\frac{da}{d\chi}\right)_e \tag{6}$$

These equations can be solved simultaneously to give a_h by noting that continuity of chemical activity is required at the stroma-epithelium interface, so that a_s at $x = h$ is equal to a_e at $x = h$. The requirement of continuity of flux at $x = h$ gives

$$D_s\left(\frac{da}{d\chi}\right)_s = D_e\left(\frac{da}{d\chi}\right)_e \tag{7}$$

For the first set of experiments, where the anterior surface ($x = L$) is covered with the PMMA lens, the condition at times later than zero is that the gradient of ion pair chemical activity is zero. Stated mathematically, this condition is

$$\left(\frac{da_e}{d\chi}\right)_{x=L} = 0 \tag{8}$$

In the non-steady state, as in the steady state, there must at all times be continuity of chemical activity and of flux at the boundary between stroma and epithelium, so we have

$$a_s(\chi = h) = a_e(\chi = h) \tag{9}$$

$$D_s\left(\frac{\partial a}{\partial \chi}\right)_s (\chi = h) = D_e\left(\frac{\partial a}{\partial \chi}\right)_e (\chi = h) \tag{10}$$

The solution of Eqs. 3 and 4, subject to the initial and boundary conditions, is a formidable task. An analytical solution is generally considered to be impossible, but finite-difference methods employing high-speed digital computation are successful. In the finite-difference scheme, a mosaic of cells replaces the continuum of the real body. Orvis has described the use of commercially available spreadsheet programs for the solution of equations of the type of 3 and 4 (Orvis, 1987). We introduced here a method for solving Eqs. 3 and 4 for a multilayered system. The method is outlined in the Appendix.

EXPERIMENTAL INPUT DATA USED FOR COMPARING EXPERIMENTAL TO MODEL RESULTS

pH data of Fig. 1 were converted to hydrogen ion chemical activity in the dye-labeled endothelial cells as a function of time after either 1) the application to the anterior surface of a tight-fitting PMMA contact lens (*open square*), or 2) the addition of bicarbonate to the medium superperfusing the anterior surface of the cornea (*closed square*). In this last case, the chemical activity of hydrogen and bicarbonate ion at $x = L$ becomes the same as at $x = 0$.

Analysis of non-steady-state diffusion data requires that the time of change of boundary condition be known. Inspection of Giasson's data indicated that the mechanism by which the boundary condition was changed could insert a delay of 40 s into the time base of his data. This 40-s delay is inserted into the time base of Giasson's data, as presented in Figs. 1 and 2. This time delay is reasonable, in view of the mechanical arrangement Giasson used.

RESULTS

A comparison of experimental results (Giasson, 1994) with predictions from a mathematical model requires the thickness of the cornea and the location of the observation point to be known. The thickness was taken to be 0.04 cm, because this is the average normal thickness of the adult rabbit cornea.

The non-steady-state diffusion equation, represented here by Eqs. 3 and 4, is conventionally solved for a single-layer system. Solutions for multiple layers have heretofore not been possible, except on large-scale computers. For a single layer in one dimension, the solution of the non-steady-state diffusion equation can be displayed on a single graph. Such graphs are displayed by Crank (1956). The vertical axis is conventionally chosen to be a nondimensional function of the initial chemical activity (or concentration), the final chemical activity, and the activity at some point and time in the system. The expression for this nondimensional chemical activity is

$$\frac{a_t - a_{t=\infty}}{a_{t=0} - a_{t=8}} \tag{11}$$

for a particular set of initial and boundary conditions.

The horizontal axis is the dimensional distance into the layer from the origin, taken as $x = 0$, to the opposite surface, taken as $x = L$. The dimensionless distance is then defined as $x = x/L$ and ranges from $x = 0$ at the origin to $x = 1$ at the opposite face. The time term in the solution of the non-steady-state diffusion equation is represented as a parameter on a series of curves in the plot of dimensionless chemical activity versus dimensionless distance. Defining a dimensionless time as

$$t' = \frac{Dt}{L^2} \tag{12}$$

allows a single graph with a family of dimensionless time curves to represent all parameters (chemical activity, layer thickness, and time) for a given set of initial and boundary conditions.

For the two-layer mathematical model of the cornea chosen for this study, no single graph can display the solution, because two additional parameters have been added. These are the ratio of the thickness of layer 1 to that of layer 2 and the ratio of the diffusion coefficient of layer 1 to that of layer 2. To make the presentation of data manageable, we have selected the best estimated histological thickness ratio of the layers and the diffusion coefficient ratio that yields the closest fit of experimental to model data. For the rabbit cornea, anatomical data lead us to believe that an epithelial thickness of 40 μm is reasonable. This makes the epithelium 10% of the total corneal thickness. We had provide little guidance for the selection of the ratio of diffusion coefficients of the H^+-HCO_3^- ion pair in the stroma and epithelium. When we make the diffusion coefficient in the epithelium 20% of that in the stroma, we obtain the best fit of experimental to model data.

The mathematical model yields Figs. 4 and 5, which show how the hydrogen-bicarbonate ion pair chemical activity changes with time when the observer is at $x = 2$ μm. The linearity of the functional relationship in the range $x = 0$ to $x = 0.20$, as shown in Figs. 4 and 5, demonstrates that there is the same fractional change in chemical activity at all points in this spatial range in any time interval. As stated earlier, this is an important observation because it means that, for the purposes of mathematical analysis of the data, the experimenter does not need to select a precise point where pH is being measured in the rabbit cornea, as long as the observation point is within 80 μm of $x = 0$.

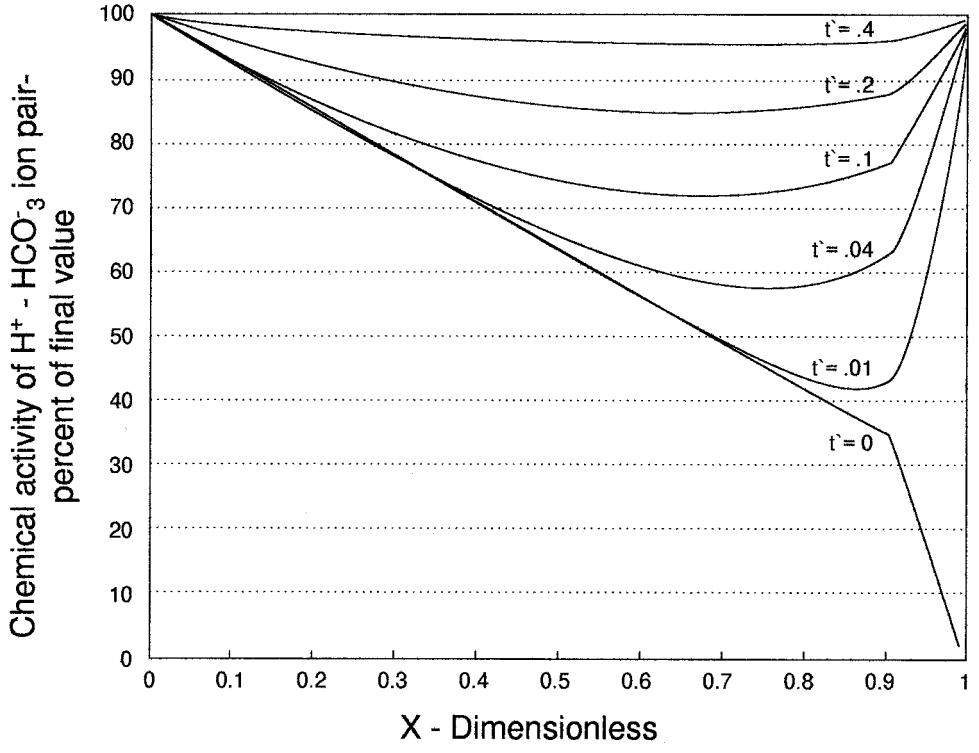

FIGURE 5 Same as Fig. 4, except that, in the case for times greater than zero, anterior and posterior surfaces are bathed by the same solution.

Another important observation is that, for an observer near $x = 0$, a single-layer cornea with the properties of the stroma will behave very much like the stroma-epithelium combination for the experiment in which the PMMA lens is applied to the anterior surface. This observation allows us to seek a match of the experimental data from the first set of experiments to the mathematical model, by selecting only the hydrogen-bicarbonate ion pair diffusion coefficient in the stroma.

DISCUSSION

Several salient features of this study can be recognized by simply inspecting the open squares of Fig. 2. Giasson's first set of experiments (Giasson, 1994), in which transfer of CO_2 out of the cornea is blocked at time 0 by a PMMA contact lens applied to the anterior surface, yields a H^+ versus time history that closely resembles results from a straightforward diffusion experiment of a single diffusing species in a homogeneous, single-layer medium. Crank, Bird et al., and others have shown how the concentration versus time curve can be distorted in the presence of complicated interactions of the diffusing substance and the medium (Crank, 1956; Bird et al., 1960). The shape of the curve in Fig. 2 is evidence for simple diffusion in our case of the hydrogen-bicarbonate ion pair in the cornea.

A second interesting feature of the curve in Fig. 2 is its time history. The experimental curve rises to 50% of its final value in 250 s. If the diffusion coefficient for the H^+-HCO_3^- ion pair were 2.5×10^{-5} cm^2/s, as is usual for these diffusing species in water, then for a layer 0.04 cm thick the curve would have reached 50% of final value in 25 s. There is clearly a retardation of the diffusion of the H^+-HCO_3^- ion pair in the stroma. This retardation is severalfold greater than would have been expected in a 78% water content neutral gel.

Crank (1956) shows that if there is an instantaneous reversible reaction of the diffusing species with the medium, then the apparent diffusion coefficient will be

$$D_{app} = \frac{D}{1 + R} \tag{13}$$

where R is the proportion of the diffusing species that is free to diffuse. If S is the concentration of immobilized diffusing species and C is the concentration that is free to diffuse, then

$$S = RC \tag{14}$$

Note that this kind of reaction of diffusing species with the fixed matrix does not change the shape of the concentration versus time curve. Only the value of the diffusion coefficient needed to fit the experimental data to the model is changed.

Our best estimate of the diffusion coefficient for the H^+-HCO_3^- ion pair in the stroma is obtained by matching the experimental data of Fig. 2, in which a PMMA contact lens is applied to the anterior surface of the cornea at time 0 to the model. The match is shown in Fig. 6. This match of the model to the experimental data is for a single-layer

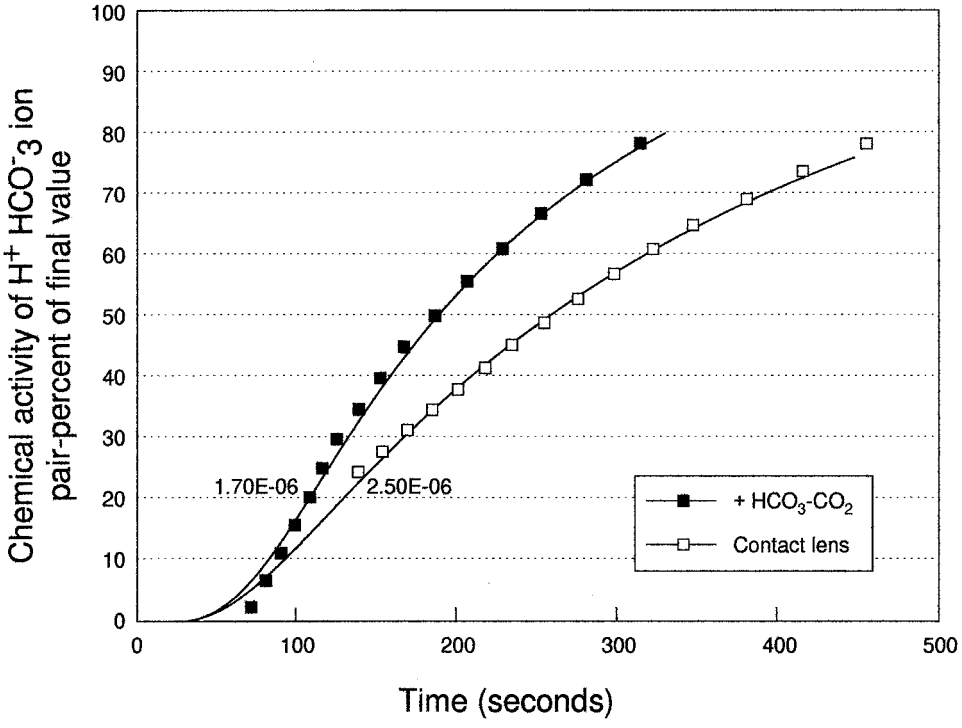

FIGURE 6 Experimental data and the computer-generated solution for both sets of experiments. □, Insertion of a contact lens over a single-layer cornea 0.04 cm thick, with a diffusion coefficient of 2.5×10^{-6} cm^2/s for the H^+-HCO_3^- ion pair. ■, Addition of 5% CO_2-HCO_3^- in the perfusate for a cornea composed of a stroma (0.0362 cm thick) of ion pair diffusion coefficient 2.5×10^{-6} cm^2/s and an epithelium (0.0038 cm thick) of ion pair diffusion coefficient 0.42×10^{-6} cm^2/s. The total thickness is 0.040 cm, and the effective diffusion coefficient is 1.7×10^{-6} cm^2/s.

cornea (all stroma) 400 μm thick and a diffusion coefficient of 2.5×10^{-6} cm^2/s for the H^+-HCO_3^- ion pair in this layer.

Newman gives the individual diffusion coefficients for H^+ and HCO_3^- in pure water at 25°C as 9.3×10^{-5} cm^2/s and 1.1×10^{-5} cm^2/s, respectively (Newman, 1991). When these diffusion coefficients are modified by the Stokes-Einstein relationship (Goldstick and Fatt, 1970) to 37°C, the temperature of Giasson's experiment, they become 12.5×10^{-5} cm^2/s for H^+ and 1.48×10^{-5} cm^2/s for HCO_3^-.

Application of the Nernst-Einstein relationship (Newman, 1991),

$$D = \frac{D_+ D_- (Z_+ - Z_-)}{Z_+ D_+ - Z_- D_-} \tag{15}$$

to Newman's individual H^+ and HCO_3^- diffusion coefficients, modified to 37°C, yields a diffusion coefficient for the H^+-HCO_3^- ion pair of 2.6×10^{-5} cm^2/s in pure water. This is one order of magnitude greater than the diffusion coefficient that best fits Giasson's experimental data to the mathematical model presented here.

There are two properties of the stroma that can reduce the diffusion coefficient of the H^+-HCO_3^- ion pair below that expected for the ion pair in pure water. First is the 20% volume fraction in the stroma that is not available for the diffusion of the H^+-HCO_3^- ion pair. However, a solution with 20% protein content reduces the diffusion coefficient of small ions or nonionic diffusing species by only twofold (Bird et al., 1960), not the tenfold reduction seen in Giasson's experiments on the stroma.

The other property of the stroma that can reduce the diffusion coefficient of the H^+-HCO_3^- ion pair are the negatively charged gels, glycosaminoglycans (GAGs), that surround the collagen fibers forming the body of the stroma (Fatt and Weissman, 1992).

The aqueous solution in equilibrium with the stromal GAGs has a salt concentration of ~175 mM. The cations of these salts are attracted to the negative charges of the GAGs and act as counterions. We are not prepared to give a quantitative explanation for the retarding effect of this counterion atmosphere on the diffusion of the H^+-HCO_3^- ion pair, but the possibility of slowing diffusion does exist.

Using Crank's expression for the reduction of the diffusion coefficient by instantaneous reaction with stromal GAGs (given here as Eq. 13), we obtain a retardation of 9.4 for diffusion of the H^+-HCO_3^- ion pair in the stroma compared to the diffusion in a nonreacting matrix (Crank, 1956). Interaction of the diffusing ion pair with the counterion atmosphere around the stromal GAGs is likely to be a more serious factor in reducing the diffusion coefficient of the H^+-HCO_3^- ion pair than a simple excluded volume effect.

Diffusion in the epithelium

In the second set of Giasson's experiments, the anterior surface is perfused with Ringer's solution in equilibrium with 5% CO_2/95% air at time 0 and thereafter. The H^+-HCO_3^- ion pair concentration curve versus time, (Fig. 2, *closed squares*) can be matched by the mathematical model by use of a single diffusion coefficient of 1.7×10^{-6} cm^2/s, as shown in Fig. 6 (*closed symbols*). In this experiment the retarding effect on the ion pair diffusion coefficient in the epithelium operates throughout the whole time period of the

experiment. We chose to derive an effective ion pair diffusion coefficient for the epithelium by using the simplistic model relating the total diffusion resistance of the two-layer system (reciprocal of diffusion) to the sum of the resistances of the stroma and epithelium. The resistance relationship can be stated as

$$\frac{L}{D(t)} = \frac{(L - L^{(e)})}{D^{(s)}} + \frac{L^{(e)}}{D^{(e)}} \tag{16}$$

where $D^{(s)} = 2.5 \times 10^{-6}$ cm^2/s; $D(t) = 1.7 \times 10^{-6}$ cm^2/s; $L^{(e)} = 0.0038$ cm; $L^{(s)} = 0.0362$ cm; $L(t) = 0.0400$ cm. Equation 16 yields the result that $D^{(e)}$ is 0.42×10^{-6} cm^2/s. In constructing the two-layer mathematical model, the assumption was made that the diffusion coefficient of the ion pair in the epithelium was 20% of that in the stroma. The simplistic model that treats the cornea as a single layer with an ion pair diffusion coefficient of 1.7×10^{-6} cm^2/s is calculated from the diffusion resistances stated above. In the simplistic model, the ion pair diffusion coefficient in the epithelium is 17% of that in the stroma. Another iteration of model building and matching the model to experimental data might reduce the difference between the assumed ratio of $D_e/D_s = 0.20$ in the model and the value of 0.17 found by a simple calculation of an assumed single layer with the properties of the two layers in series. The precision of the experimental data is too low to warrant any such further manipulation of the model. A rounded value of 0.4×10^{-6} cm^2/s for the ion pair diffusion coefficient in the epithelium is offered here as the best estimate.

The complex structure of the five-cell-thick epithelium precludes any call upon structure as an explanation for the observed diffusion coefficient (Hogan et al., 1971). The epithelial cell structure is very heterogeneous. About one-third of the volume of each cell is occupied by a nucleus; the remainder is cytoplasm. The cytoplasm is a dilute gel of 70–80% water; the remainder is protein strands. The nucleus in the living cell is continually changing. A thin nuclear membrane surrounds a dilute solution of complex proteins. We are unable to relate the structure of the epithelial cell to the observed diffusion coefficient of the H^+-HCO_3^- ion pair in these cells.

Single-ion diffusion coefficients

The single ion diffusion coefficients, $D(H^+)$ and $D(HCO_3^-)$, are only hypothetical quantities because electroneutrality requires that H^+ and HCO_3^- diffuse together in Giasson's experiment. Nevertheless, $D(H^+)$ and $D(HCO_3^-)$ are valuable quantities because they can be compared among various tissue structures to examine the effect of structure on ion mobility.

The H^+-HCO_3^- ion pair diffusion coefficients at 37°C calculated from Giasson's data can be converted to single ion diffusion coefficients, if it is assumed that the ratios of the single ion diffusion coefficients in the stroma and epithelium are the same as in water. Newman gives the ratio $D(HCO_3^-)/D(H^+)$ in pure water at 25°C as 0.119 (Newman, 1991). The ratio will be the same at other temperatures if we assume that the Stokes-Einstein relationship applies equally to HCO_3^- and H^+. If we substitute $D(H^+) = 8.26\ D(HCO_3^-)$ from Newman's ratio into the Nernst-Einstein equation (Eq. 15), we obtain $D(H^+) = 11.8 \times 10^{-6}$ cm^2/s and $D(HCO_3^-) = 1.5 \times 10^{-6}$ cm^2/s at 37°C in the stroma.

A similar calculation for the epithelium, using 0.4×10^{-6} cm^2/s as the ion pair diffusion coefficient in this layer, yields $D(HCO_3^-) = 0.22 \times 10^{-6}$ cm^2/s and $D(H^+) = 1.9 \times 10^{-6}$ cm^2/s.

Several comparisons can be made from the ion pair and the single ion diffusion coefficients. For the ion pair H^+-HCO_3^-, the ratio of diffusion coefficient in stroma to epithelium is 6.3. The ratio of diffusion coefficient in stroma to epithelium for the single ion is 7.9, whereas the ratio for the single bicarbonate ion is 8.6. These results tend to show that the tissue structure has a greater influence on mobility than the nature of the diffusion entity, H^+, HCO_3^-, or the ion pair.

If we compare the mobility of the ion pair to the single ion mobilities, we find that the ratio of $D(H^+)$ to D(ion pair) is 4.7–4.8 for both stroma and epithelium.

CONCLUSIONS

A mathematical model of the cornea that treats this tissue as a one-dimensional two-layer system (stroma and epithelium) has allowed us to compare experimentally observed pH transients with predictions from the model. We arrive at an estimate for the diffusion coefficients of the H^+-HCO_3^- ion pair in the stroma and epithelium. For the stroma, we find the diffusion coefficient of the ion pair at 37°C to be 2.5×10^{-6} cm^2/s. In the epithelium, the diffusion coefficient of the ion pair at 37°C is 0.4×10^{-6} cm^2/s.

For the individual ion diffusion coefficients, we estimate that at 37°C in the stroma $D(H^+) = 11.8 \times 10^{-6}$ cm^2/s and $D(HCO_3^-) = 1.5 \times 10^{-6}$ cm^2/s. For the epithelium at 37°C we estimate $D(H^+) = 1.9 \times 10^{-6}$ cm^2/s and $D(HCO_3^-) = 0.22 \times 10^{-6}$ cm^2/s.

APPENDIX: MATHEMATICAL MODEL OF THE STROMA-EPITHELIUM SYSTEM USED IN THE COMPUTER CALCULATION

The equations representing transient diffusion in the stroma and epithelium, when put in dimensionless form, are identical to the equations governing conductive heat flow in a multilayered material. Much research has gone into the solution of these heat equations constrained by a variety of boundary conditions, dealing mostly, however, with single-layered material. Parts of that methodology were applied to the study of the stroma-epithelium system given here. Carslaw and Jaeger report on the solution of the transient behavior of heat flow in a single-layer system that they achieved by evaluating analytic functions (Carslaw and Jaeger, 1959). We, in turn, evaluated finite-difference equations to obtain solutions to the differential equations. As a basis for proceeding to the study of multilayered systems, we ran our finite-difference model in the single-layer mode with the same boundary conditions as shown in the example by Carslaw and Jaeger (1959, p. 98, figure 10 *b*). The values produced by our computer

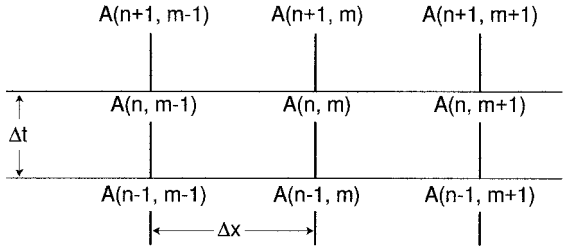

FIGURE 7 Finite-difference scheme used to divide the tissue into computational cells. The differential equations for diffusion now become separately applicable to each cell.

solution agreed with those shown in their figure 10 within the accuracy permitted by reading their graph.

As mentioned above, the unique problem in solving the differential equations for non-steady-state diffusion is the fact that one must represent two media with different thicknesses and diffusion coefficients in the stroma-epithelium system. Where the two media meet, thermodynamics require that the activity at the interface must be the same as that calculated from both sides of the interface. This requires that the interface value change with time, as dictated by what is happening in the separate media. From a review of the heat and chemical diffusion literature, we could not determine where such multilayered systems had been evaluated with the use of the analytic functions or the finite-difference approach reported here.

The basic concept of our mathematical model is to represent the partial derivatives in the diffusion equation as a set of finite-difference equations. To understand the computing method, one should visualize a network of points in which each point is located at discrete values x and t'. These values of x and t' are achieved by incrementing time and the distance coordinate by quantities called Δt and Δx. The number of times that Δt has been incremented is indicated by the variable n, and the number of increments in Δx is indicated by the variable m. The chemical activity values for the ion pair H^+-HCO_3^- are known at $t' = 0$ for all space points and are known at all times for the boundary space points $x = 0$ and $x = L$ for some experimental cases or the value of the space derivative of chemical activity with respect to x at the boundary at $x = L$ for other experimental cases.

The computing method starts its calculation at $t' = 0$, where the chemical activity values are known at all space points, and marches the solution forward through time until the system reaches some desired condition of chemical activity level or time. Sets of activity values can be sampled along the way. A diagram of the finite-difference scheme is shown in Fig. 7. The notation used is as follows:

$A(n, m)$ = activity at time n and space m. These values are referred to as being at the back time line.

$A(n + 1, m)$ = activity at time $n + 1$ and space m. These values are referred to as being at the forward time line.

Δt = increment in time; Δx = increment in space; D = diffusion coefficient.

The average of the finite-difference representation at the forward time line and the back time line is as follows:

$$D\left(\frac{\partial^2 A}{\partial x^2}\right)_{(n+1/2,m)} = \left(\frac{A(n, m-1) + A(n+1, m-1)}{2(\Delta x)^2}\right) - \left(\frac{A(n, m) + A(n+1, m)}{(\Delta x)^2}\right) + \left(\frac{A(n, m+1) + A(n+1, m+1)}{2(\Delta x)^2}\right)$$

which, in turn, is equal to the time derivative as follows:

$$\left(\frac{\partial A}{\partial t}\right)_{(n+1/2,m)} = \left(\frac{A(n+1, m) - A(n, m)}{\Delta t}\right)$$

Recognizing the fact that we know the values of activity at the back time line, the equations derived above provide a set of algebraic equations where each unknown activity has two neighbors, each related implicitly to it, and three values at the back time line explicitly related to it. The coefficients of these algebraic equations, when put in matrix form, provide a matrix with a strong diagonal and coefficients closely clustered on both sides. Fig. 8 gives a visual picture of this matrix. We found the matrix solution method given by Bruce et al. (1953) to be stable and accurate with a variety of input numbers.

To derive the finite-difference equation at the interface between two materials with different diffusion coefficients, such as the stroma and epithelium, we return to the original difference equations that we used to derive the partial difference equations. We know from Fick's law of diffusion that the quantity of material diffusing is proportional to the activity gradient. Thus, with D2 representing the diffusion coefficient of the stroma and D1 representing the diffusion coefficient of the epithelium:

$$Q2 = D2*(A(n, m) - A(n, m-1))/\Delta x$$

$$Q1 = D1*(A(n, m+1))/\Delta x$$

$$(Q2 - Q1)/\Delta x = \partial A/\partial t^{\sim}$$

If this equation is averaged with its counterpart at the forward time line, we obtain the finite-difference representation at the interface. It should be stated that we have assumed that the interface passes directly through the center of the Δx box.

$$\begin{aligned} &D2*(\Delta t^{\sim}/(2*\Delta x \wedge 2)*A(n+1, m-1) \\ &\quad + ((D2 + D1)*(\Delta t^{\sim}/(2*\Delta x \wedge 2) - 1)*A(n+1, m) \\ &\qquad + D1*(\Delta t^{\sim}/(2*\Delta x \wedge 2))*A(n+1, m+1) \\ &= D2*(\Delta t^{\sim}\, x \wedge 2)*A(n, m-1) \\ &\quad + ((D2 + D1)*(\Delta t^{\sim}/(2*\Delta x \wedge 2) - 1*A(n, m-1) \\ &\qquad + D1*(\Delta t^{\sim}/(2*\ \Delta x \wedge 2)*A(n, m+1) \end{aligned}$$

To derive the finite-difference equation at the stroma boundary (posterior corneal surface), where we wish to hold the activity constant, we assume that a point located externally at $\Delta x/2$ distance from the boundary can be averaged with the activity value at increment 1, and that average is equal to the fixed boundary condition, which in our case is the variable BCS.

$$\mathrm{BCS} = (A(n, 0) = A(n, 1))/2$$

$$A(n, 0) = 2*\mathrm{BCS} - A(n, 1)$$

The finite-difference representation of space point 1 is then

$$\begin{aligned} &((-3*D2*\ \Delta t^{\sim}/(2*\Delta\, x \wedge 2)) - 1)*A(n+1, 1) \\ &\qquad + D2*(\Delta t^{\sim}/(2*(\Delta t^{\sim}/2*\Delta\, x \wedge 2))*A(n+1, 2) \\ &= -4*D2*(\Delta t^{\sim}/(2*\Delta x \wedge 2)*\mathrm{BCS} \\ &\quad + ((3*D2(\Delta t^{\sim}/(2*\Delta x \wedge 2) - 1)*A(n, 1) \\ &\quad + D2*(\Delta t^{\sim}/(2*\Delta x \wedge 2))*A(n, 2) \end{aligned}$$

Using the same reasoning, a similar-finite difference equation can be derived for the space point at the epithelium boundary where BCE is the value of the fixed boundary condition.

$$\begin{vmatrix} b(n,1) & c(n,1) & & & \\ a(n,2) & b(n,2) & c(n,2) & & \\ & a(n,3) & b(n,3) & c(n,3) & \\ & & a(n,4) & b(n,4) & c(n,4) \\ & & & & \\ & & a(n,M-1) & b(n,M-1) & c(n,M-1) \\ & & & a(n,M) & c(n,M) \end{vmatrix} * \begin{vmatrix} A(n+1,1) \\ A(n+1,2) \\ A(n+1,3) \\ A(n+1,4) \\ \\ A(n+1,M-1) \\ A(n+1,M) \end{vmatrix} = \begin{vmatrix} d(n,1) \\ d(n,2) \\ d(n,3) \\ d(n,4) \\ \\ d(n,M-1) \\ d(n,M) \end{vmatrix}$$

FIGURE 8 The computational matrix used to compute activity in each cell as a function of time.

At the epithelial boundary (anterior cornea), where a no flow boundary condition is to be imposed by applying the PMMA contact lens, a finite-difference equation can be derived using

$$A(n, M) = A(n, M + 1)$$

and

$$A(n + 1, M) = A(n + 1, M + 1)$$

where M is the total number of space increments.

The use of the Lotus 123 spreadsheet system to solve for one time step is a straightforward calculation. The process is to place the back time line activities in a spreadsheet column. The forward time line activities are calculated through a series of column calculations, and the results are placed in a separate column. Using the Lotus command/RV(solution column) ~ (original column) ~ the solution values are placed in position to repeat the calculation and thus advance the calculation by one time step.

INPUT VALUES TO BE MEMORIZED					CALCULATED VARIABLES				
$L=	1.00	$NUMBER=	10.00		TO BE MEMORIZED				
$DTWO=	1.00			$YC=	62.50				
$DONE=	0.20	$XSTART=	0.00	$DX=	0.10	=($L/$NUMBER)			
$YSINIT=	100.00	$XEND=	1.00	$RA=	0.0625	=(+$DT/(2*$DX^2))			
$YEINIT=	0.00	$XC=	0.75						
$BCS=	100.00	=BOUND.COND.STROMA							
$BCE=	100.00	=BOUND.COND.EPITH.							
X AXIS	A(n)	a	b	c	d	w	g	p	A(n+1)
0.050	97.67	0.00	-1.19	0.06	-110.17	-1.19	92.78	91.18	97.68
0.150	93.06	0.06	-1.13	0.06	-93.07	-1.12	88.14	78.43	93.08
0.250	88.63	0.06	-1.13	0.06	-88.65	-1.12	83.95	75.38	88.67
0.350	84.51	0.06	-1.13	0.06	-84.54	-1.12	80.06	76.15	84.57
0.450	80.89	0.06	-1.13	0.06	-80.94	-1.12	76.63	78.09	80.98
0.550	77.98	0.06	-1.13	0.06	-78.03	-1.12	73.85	80.98	78.09
0.650	76.00	0.06	-1.13	0.06	-76.08	-1.12	71.95	84.57	76.15
0.750	75.21	0.06	-1.08	0.01	-75.30	-1.07	74.47	88.67	75.38
0.850	78.18	0.01	-1.03	0.01	-78.30	-1.02	77.31	93.08	78.43
0.950	91.05	0.01	-1.04	0.00	-93.62	-1.04	91.18	97.68	91.18
INPUT VARIABLES			X AXIS	Y@t~=0	Y@t~=$T	\B	/RV		
TO BE MEMORIZED		$DT GUIDE=	0.000	100.00	100.00		J11..J20		
$TSTART=	0.00000	$DX*$DX/2	0.050	97.50	97.68		~B11..B20~		
$DT=	0.00125	0.00500	0.150	92.50	93.08		{let $NCOUNT,$NCOUNT+1}		
$NSTOP=	5000		0.250	87.50	88.67		{let $T,$T+$DT}{calc}		
$TSTOP=	0.10000		0.350	82.50	84.57		{if $T>=$TSTOP}{calc}{beep}{quit}		
			0.450	77.50	80.98		{branch \B}		
CALCULATED VARIABLES			0.550	72.50	78.09				
TO BE MEMORIZED			0.650	67.50	76.15	\C	/WGRC		
$NCOUNT=	80		0.750	62.50	75.38		/RV		
$T=	0.10000		0.850	37.50	78.43		E24..E33~		
			0.950	12.50	91.18		B11..B20~		
			1.000	0.00	100.00		{let $T,$TSTART+$DT+1E-10}		
							{let $NCOUNT,1}		
							{calc}		
							{calc}		
							{quit}		

FIGURE 9 Spreadsheet snapshot of demonstration 10-cell model at dimensionless time of 0.1.

This whole process is achieved through a macro that we have labeled "\[B]". The setting of original values to start the calculation is achieved with another macro command named "*C*".

The status of a spreadsheet calculation of a 10 model (10 cells) at a dimensionless time of 0.1 is presented in Fig. 9. The 10-increment model was chosen to display the basic concepts, but the results of its calculations were not used in this paper. All results presented here were developed with a 100-cell model.

NOTES ON LOTUS 123 PROGRAM

The spreadsheet provides hints on how to set up a particular problem. For example, a variable is memorized by putting the cell pointer on a cell containing that variable and then executing the command/RNC and then the variable name. As a reminder, we have placed the variable's name in the cell immediately to the left of the memorized cell. The symbol $ as the first character in a variable name indicates to the Lotus system that the variable is memorized.

The heart of the program is the liberal use of Lotus 123 macro commands. After a macro is typed in, it must be activated. We have coined the title of "arming the macro" for the process. Arming is achieved by putting the cell pointer on the macro label, such as \[B], and then executing the command/RNLR. When the macro itself must be executed, the ALT key is depressed along with the designated letter key.

The spreadsheet is set to stop iterating when a time called $TSTOP is achieved. With this break in the calculation, one can store the results at that time. In the 100-cell model, a series of macros provided this data capture ability. Note that the calculation is also set to stop at the value of the variable $NCOUNT, which is the number of iterations done in the calculation. Obviously, one must set the value of the nonstopping variable to be greater than the desired stopping variable.

A floppy-disk copy of the 100-cell model program is available upon request (from TDM; E-mail address: thomas_d_mueller@msn.com).

This paper is dedicated to the memory of Professor Fatt, who passed away on October 5, 1996.

REFERENCES

Bird, R., W. Stewart, and E. Lightfoot. 1960. Transport Phenomena. Wiley, New York.

Bonanno, J. A., and C. J. Giasson. 1992. Intracellular pH regulation in fresh and cultured bovine corneal endothelium. I. Na^+/H^+ exchange in the absence and presence of HCO_3^-. *Invest. Ophthalmol. Vis. Sci.* 33: 3058–3067.

Bonanno, J. A., and T. E. Machen. 1989. Intracellular pH regulation in basal corneal epithelial cells measured in corneal explants: characterization of Na/H exchange. *Exp. Eye Res.* 49:129–142.

Bruce, G. H., D. W. Peaceman, and H. H. Rachford Jr. 1953. Calculation of unsteady-state gas flow through porous media. *Trans. AIME.* 151: 79–92.

Carslaw, H. S., and J. C. Jaeger. 1959. Conduction of Heat in Solids, 2nd Ed. Oxford University Press, Oxford.

Conroy, C. W., R. H. Buck, and T. H. Maren. 1992. The microchemical detection of carbonic anhydrase in corneal epithelia. *Exp. Eye Res.* 55:637–640.

Crank, J. 1956. Mathematics of Diffusion. Oxford University Press, Oxford.

Davenport, H. 1958. The ABC of Acid-Base Chemistry, 4th Ed. University of Chicago Press, Chicago.

Fatt, I., and B. Weissman. 1992. Physiology of the Eye, 2nd Ed. Butterworth-Heinemann, Boston.

Giasson, C. J. 1994. Effects of contact lens wear and lactate transport on corneal epithelial and endothelial intracellular pH. PhD Dissertation. University of California, Berkeley, CA.

Giasson, C. J., J. A. Bonanno, and I. Fatt. 1995. CO_2 tension in the rabbit anterior segment during simulated eye closure. *Invest. Ophthalmol. Vis. Sci.* 36:S311.

Goldstick, T., and I. Fatt. 1970. Diffusion of oxygen in solutions of blood proteins. *Chem. Eng. Prog. Symp. Ser.* 66:101.

Hogan, W., J. Alvarado, and J. Weddell. 1971. Histology of the Human Eye. Saunders, Philadelphia.

Klyce, S., H. Neufeld, and J. Zadunaisky. 1973. The activation of chloride transport by epinephrine and Db cyclic-AMP in the cornea of the rabbit. *Invest. Ophthalmol. Vis. Sci.* 12:127–139.

Newman, J. 1991. Electrochemical Systems, 2nd Ed. Prentice Hall, Englewood Cliffs, NJ.

Orvis, W. 1987. 1–2-3 for Scientists and Engineers. Sybex, San Francisco.

Wistrand, P. J., M. Schenholm, and G. Lonnerholm. 1986. Carbonic anhydrase isosymes CA I and CA II in the human eye. *Invest. Ophthalmol. Vis. Sci.* 27:419–428.